Talanta 120 (2014) 443–449

Contents lists available at ScienceDirect

Talanta

journal homepage: www.elsevier.com/locate/talanta

Humidity and temperature sensing properties of copper oxide–Si-adhesive nanocomposite

Sher Bahadar Khan [a,b], Muhammad Tariq Saeed Chani [a,d,*], Kh. S. Karimov [c,d], Abdullah M. Asiri [a,b], Mehran Bashir [c], Rana Tariq [c]

[a] Center of Excellence for Advanced Materials Research (CEAMR), King Abdulaziz University, P.O. Box 80203, Jeddah 21589, Saudi Arabia
[b] Department of Chemistry, Faculty of Science, King Abdulaziz University, P.O. Box 80203, Jeddah 21589, Saudi Arabia
[c] GIK Institute of Engineering Sciences and Technology, Swabi, KPK, Topi 23640, Pakistan
[d] Physical Technical Institute of Academy of Sciences, Rudaki Ave.33, Dushanbe 734025, Tajikistan

ARTICLE INFO

Article history:
Received 5 August 2013
Received in revised form
13 November 2013
Accepted 30 November 2013
Available online 10 December 2013

Keywords:
Copper oxide
Low temperature synthesis
Nanosheets
Structural properties
Humidity sensor
Temperature sensor.

ABSTRACT

Smart and professional humidity and temperature sensors have been fabricated by utilizing copper oxide–Si-adhesive composite and pure copper oxide nanosheets. Copper oxide nanosheets are synthesized by low temperature stirring method and characterized by field emission scanning electron microscopy, which reveals that synthesized product is composed of randomly oriented nanosheets, which are grown in high density with an average thickness of $\sim 80 \pm 10$ nm. X-ray diffraction confirms that the grown nanosheets consist of well crystalline monoclinic CuO. X-ray photoelectron spectroscopy and Fourier transform infrared (FTIR) spectroscopy also confirm that the synthesized nanomaterial is pure CuO without any impurity. The fabricated sensors exhibit good temperature sensitivity of $-4.0\%/^{\circ}C$ and $-5.2\%/^{\circ}C$ and humidity sensitivity of $-2.9\%/\%RH$ and $-4.88\%/\%RH$, respectively for copper oxide–Si-adhesive composite and pure copper oxide nanosheets. The average initial resistance of the sensors is equal to 250 MΩ and 55 MΩ for the composite and pure copper oxide based sensors, respectively.

1. Introduction

Humidity and temperature are the important factors which affect not only the human life but also the wild life, agriculture, storage, industrial products and manufacturing processes [1–3]. Therefore monitoring and control of humidity is very essential for better human life, good agriculture, controlled industrial processes, corrosion control and for the storage of food and industrial products [4–8]. Like humidity monitoring and control of temperature is also very essential for augmentation of industrial process and improvement of quality of life. Currently, the demand for multifunctional sensors is increasing because of integration of systems [3,9,10]. These types of sensors have many advantages like small size (single sensor replaces various sensors), reduces the use of contact leads and information can be collected from exactly same location [3].

Conventionally for the measurement of relative humidity thin plates of piezoelectric quartz and micro-porous thin films are used and their working principle is based on change in oscillation frequency and the change in luminescence respectively. The humidity can also be measured by using such type of materials which show variation of resistance or capacitance with change in humidity [11]. These materials include the polymers, ceramics and composites. Humidity sensors are also classified as resistive, capacitive, gravimetric, hydrometric, integrated and optical type sensors depending upon their basic sensing principle. For humidity sensors, nature of sensing material and the design of sensor are considered important parameters which affect the performance of sensors. Moreover high sensitivity, linear response, short response and recovery time, low hysteresis, physical and chemical stability, wide sensing range and low cost are the required properties for a best sensor [5,12,13]. To achieve these properties many types of organic, inorganic and composite materials have been investigated. From last few decades organic–inorganic nano-composites are considered as new class of material that is suitable for advanced electronic, magnetic or optic applications [14]. Due to their low density, high flexibility, easy processing and simple fabrication technology, organic materials are very attractive for electronic devices, while the only problem with organic material is their lower stability as compared to inorganic materials. It is desirable to fabricate such type of devices which have combined advantages of organic and inorganic materials. Keeping in view the above mentioned advantages, copper oxide and silicon adhesive nano-composite is used for the fabrication of humidity sensors.

* Corresponding author at: Center of Excellence for Advanced Materials Research (CEAMR), King Abdulaziz University, Jeddah 21589, P.O. Box 80203, Saudi Arabia. Tel.: +966 26 952293.
E-mail addresses: tariqchani1@gmail.com, tariqchani@hotmail.com (M.T.S. Chani).

0039-9140/$ - see front matter © 2013 Elsevier B.V. All rights reserved.
http://dx.doi.org/10.1016/j.talanta.2013.11.089

Being a p-type semiconductor cupric oxide (CuO) has energy band gap of 1.2 eV [15]. This is very attractive for researchers because of its potential applications in sensing, catalysis, solar cells and field emission. As for as sensing applications are concerned the cupric oxide may be used for sensing of various types of gases (e.g. H_2S, CO, NO_2 etc), chemicals, temperature and humidity [16–18]. Hsueh et al. fabricated humidity sensors by growing copper oxide nano wires on glass substrates [11]. They reported that resistance of the sensors increases with increase in relative humidity, while the longer nano wires show better sensitivity than smaller wires. With change in humidity from 20% to 90% the resistance increases from 0.55 MΩ to 0.62 MΩ, while the impedance increases from 6.5×10^5 to 7.7×10^5 and it is argued that this increase in resistance with increase is humidity is due to p-type semiconducting nature of copper oxide. It is also described that at 80%RH and applied bias of 5 V, the increase in temperature from 20 °C to 80 °C causes to decrease resistance of the sensors from 2.99×10^6 MΩ to 0.61×10^6 MΩ. Qi et al. fabricated humidity sensors by depositing Kcl-doped Cu–Zn/CuO–ZnO nano particles film (10 μm thick) on to five pairs of Ag–Pd integrated electrodes and compared them with sensors fabricated by un-doped Cu–Zn/CuO–ZnO [19]. It is reported that sensor fabricated by doped material have higher detection limit and more linear response as compared to sensors of un-doped material. The impedance of the Kcl doped sensors decreases by four orders of magnitude on increase in humidity from 11% to 95%.

Depending on the development of synthetic method, the nanomaterials can be produced in various sizes, compositions and morphologies. On the base of morphology nanomaterials are classified as nanotubes, nanopowders, nanorods, nanobats, nanoflowers and nanosheets etc. As the CuO and ZnO are the widely used semiconducting materials and are being studied in various nanostructured form especially nanosheets for various applications like solar cells, supercapacitor, anode for lithium ion batteries, metal ion uptake and sensing [20–25]. Liu et al. and Huang et al. fabricated CuO and ZnO nanosheets on a copper substrate respectively. These nanosheets were applied as an anode material in lithium-ion batteries for energy storage. The discharge capacities of CuO nanosheets anode is 442 $mAhg^{-1}$ at current density of 200 mAg^{-1} after 40 cycles, while that of ZnO nanosheets is 400 $mAhg^{-1}$ at 500 mAg^{-1} after 100 cycles [22,26]. Regarding humidity and temperature sensing of CuO nanosheets, it is very difficult to find any publication in the literature. Probably, it is first time that we are reporting humidity and temperature sensing properties of CuO nanosheets.

Silicon adhesives are non toxic, hydrophobic and biocompatible flexible macromolecular chains with ultra low glass transition temperature and have good chemical and thermal stability and resistance for photo-ageing. These adhesives in contact with polar surfaces undergo polar interactions and this property makes them attractive material for a verity of technical applications [27,28].

The present study is the continuation of our effort for the development of various types of sensors for environmental and electromechanical applications [12,13,29–31]. The fabricated sensors may be used as humidity as well as temperature sensing element in the devices, which are used for environmental monitoring and industrial applications.

2. Experimental

2.1. Synthesis of copper oxide nanosheets

The entire chemicals were purchased from Sigma Aldrich and used as received without further purification. The copper oxide nanosheets were synthesized according to the procedure published elsewhere [21,32,33]. In a typical reaction process, 0.1 mol L^{-1} aqueous solution of $CuCl_2$ titrated with NH_4OH solution until the pH of the solution turn out to be above 10. The ensuing solution was further stirred at 80 °C for 12 h. After terminating the reaction, black precipitate was obtained and washed with a mixture of distilled water and ethanol, sequentially and dried at room-temperature. The dried product was then calcined at 400 °C for 5 h.

2.2. Characterization of copper oxide nanosheets

The synthesized product was characterized by various techniques. The surface morphology of the synthesized CuO was investigated by field emission scanning electron microscopy (JEOL FE-SEM, Japan). The structural characterization was performed by X-ray diffraction (XRD) pattern using a PANalytical X'pert pro with Cu-Kα radiation of $\lambda=1.5406$ Å in the 2θ range from 15 to 90. The composition and optical properties of the synthesized CuO nanosheets were analyzed by using FTIR spectroscopy (Perkin Elmer, spectrum 100) and UV–visible spectroscopy (PerkinElmer, Lambda 950), respectively. The DC resistivity–temperature dependence measurements were carried out using two points probe technique (Scientific Equipment & Services) in the temperature range from room temperature to 573 K.

2.3. Fabrication and characterization of sensors

For fabrication of the sensors, copper oxide–silicone adhesive composite is prepared by mixing the powder of copper oxide (CuO) nanosheets with silicon adhesive (1:1 wt). Mixing is carried out by using mortar and pestle. Medical glass slides are used as substrate. Prior to the deposition of copper electrodes by vacuum thermal evaporation, substrates are cleaned by methanol and then dried. The length of 50 nm thick electrodes is 20 mm while the gap between two electrodes is 40 μm. The composite films of 100 μm thickness are deposited in to the gap between electrodes by using drop casting and doctor blade technology in sequence. The pellets of pure copper oxide nano-powder are also fabricated at a pressure of 300 bar by using hydraulic press. Thickness and diameter of the pellets is 0.75 mm and 12.5 mm, respectively. Terminals of the sensors are connected by the silver paste. The schematic diagrams of the fabricated sensors and pellets are shown in Fig. 1(a) and (b), respectively. After drying at room temperature conditions for 2 days, samples are annealed at 90 °C for 2 h. The indigenously made temperature and humidity setups are used for the characterization of samples. The construction detail of humidity setup is described in Refs. [5,12,29]. The FLUKE 87 multi-meter and Fisher Scientific hygrometer are used for the measurement of temperature and humidity respectively, while the Agilent U1732 LCR meter is used for the measurement of capacitance and resistance.

3. Results and discussion

3.1. The structural and optical characterization of CuO nanosheets

Typical FESEM images which are described in Fig. 2(a) and (d) are used to examine the morphology of the synthesized product. The low and high magnification FESEM images show that the synthesized products are composed of randomly grown smooth surface nanosheets, which are grown in large quantity with an average thickness of $\sim 80\pm10$ nm. The EDS analysis of copper oxide nanosheets is shown in Fig. 3, which confirms the presence of Cu and oxygen and there is no third element as an impurity.

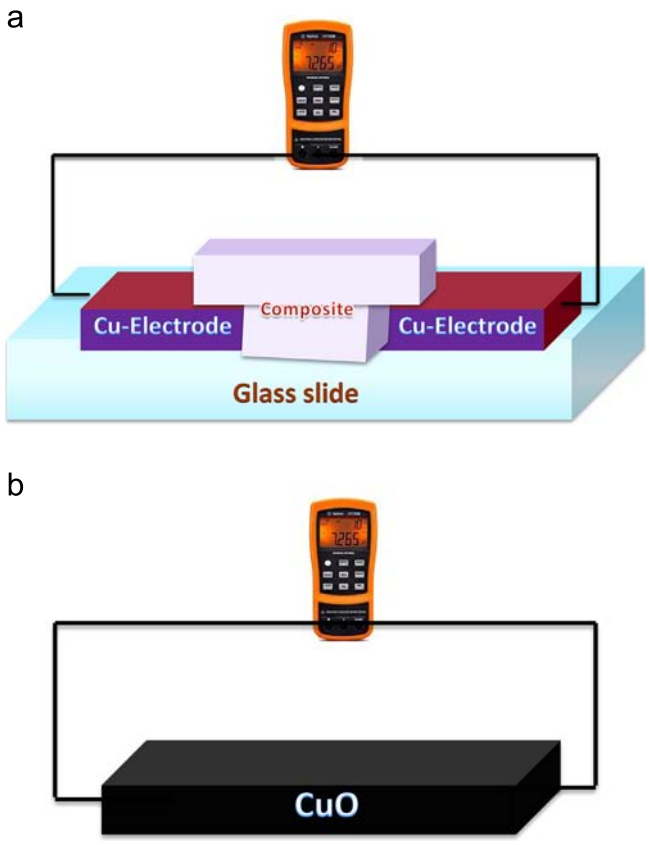

Fig. 1. The schematic diagrams of the fabricated sensors (a) and pellets (b).

The crystallinity and crystal phases of the synthesized nanosheets are elucidated by XRD pattern, which is shown in Fig. 4(a). The XRD pattern is verified by PDF cards (41-0254), which confirm that the synthesized product is base centered monoclinic CuO with a space group of $C_{2/c}$ and lattice constants of $a=4.685$ Å, $b=3.423$ Å and $c=5.132$ Å. The high intensity peaks in the XRD pattern clearly reflect the crystallinity of CuO. The chemical composition of copper oxide nanosheets was investigated by FTIR spectroscopy. Fig. 4(b) indicates FTIR spectrum which exhibited absorption bands at 504, 604, 1622, and 3472 cm^{-1}. The characteristic absorption bands at 604 and 504 cm^{-1} are responsible for Cu–O stretching vibration and the absorption bands at 3472 and 1622 cm^{-1} are due to the stretching and bending vibrational modes of absorbed water, which is normally absorbed by nanocrystalline materials from environment due to their high surface-to-volume ratio [21]. For optical characterization of CuO nanosheets, UV–vis absorption spectrum was examined and shown in Fig. 4(c). The CuO nanosheets exhibited absorption peak at 275 nm which is attributed to monoclinic CuO.

3.2. Electrical characterization of sensors

Fig. 5(a) and (b) shows resistance–temperature relationships for the composite and pure copper oxide. It can be seen that the initial resistances of copper oxide-silicon adhesive composite and pure copper oxide are on average 250 MΩ and 55 MΩ, respectively. For change in temperature from 25 °C to 80 °C, the change in resistance is 41 and 55 times in composite and pure copper oxide based sensor correspondingly, while the average change in resistance is 4.4 MΩ/°C and 1.15 MΩ/°C accordingly. The sensitivity

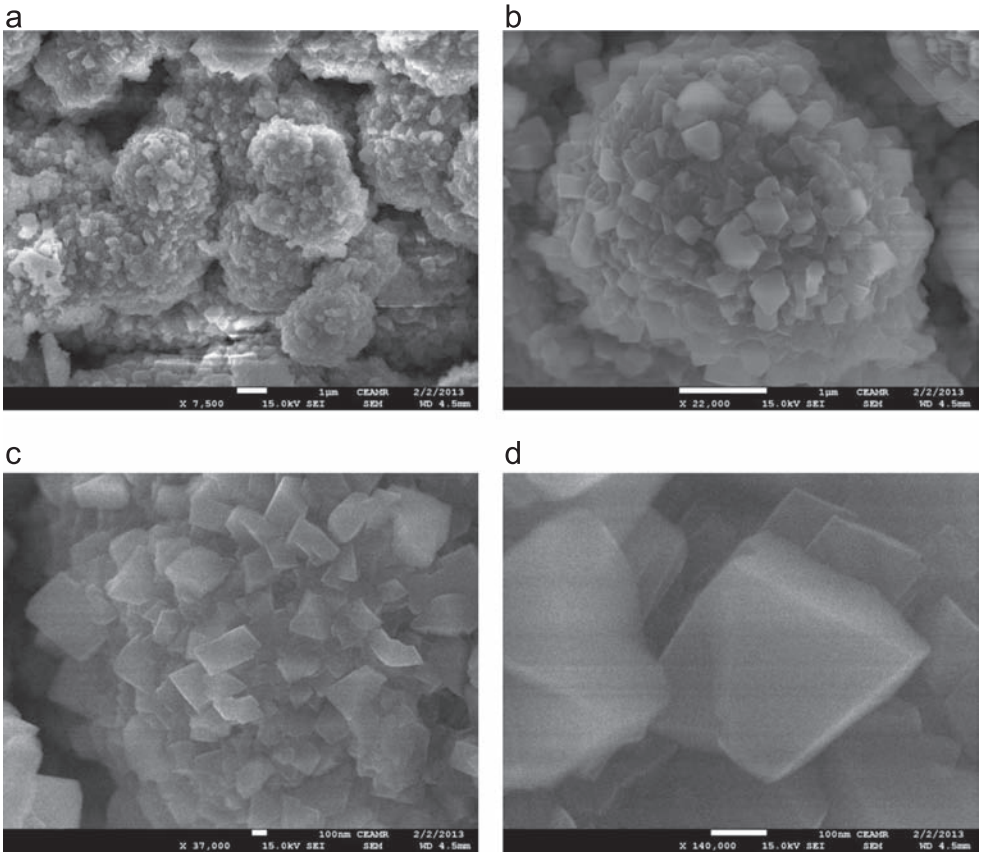

Fig. 2. The FESEM images of synthesized nano-copper oxide at various magnifications.

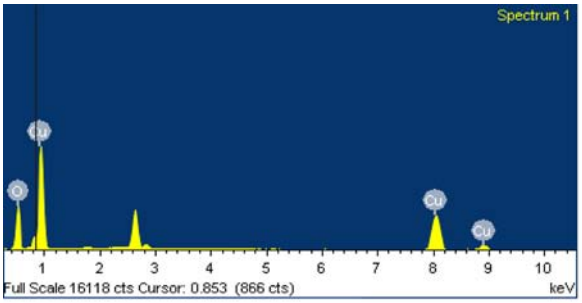

Element	Weight%	Atomic%
O K	29.86	62.83
Cu K	70.14	37.17
Totals	100.00	

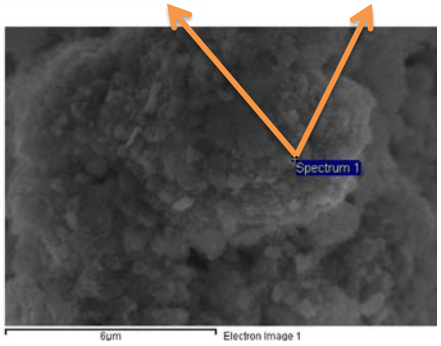

Fig. 3. EDS analysis of copper oxide nano-sheets.

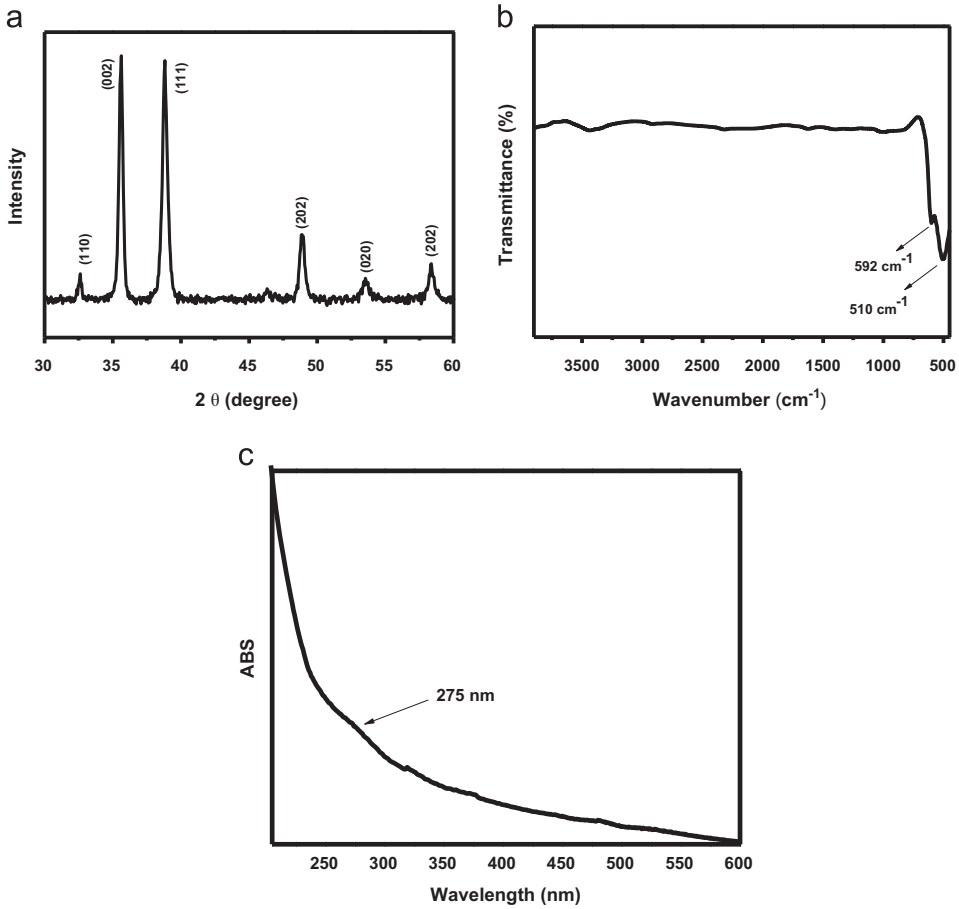

Fig. 4. XRD pattern (a), FTIR (b) and UV (C) spectra of synthesized copper oxide nano-sheets.

(S) of the sensors is determined by the following expression [34]:

$$S = (\Delta R/R_o \Delta T)100 \quad (1)$$

where R_o, ΔR and ΔT represent the initial resistance, change in resistance and change in temperature, respectively. The calculated sensitivity of the temperature sensors is up to $-4.0\%/^{\circ}C$ and $-5.2\%/^{\circ}C$ for the composite and pure copper oxide correspondingly. The sensitivity of the semiconductor temperature sensors, thermistors, typically are in the range of $-3\%/^{\circ}C$ to $-5\%/^{\circ}C$ [35], that is actually coincide with sensitivity of the investigated

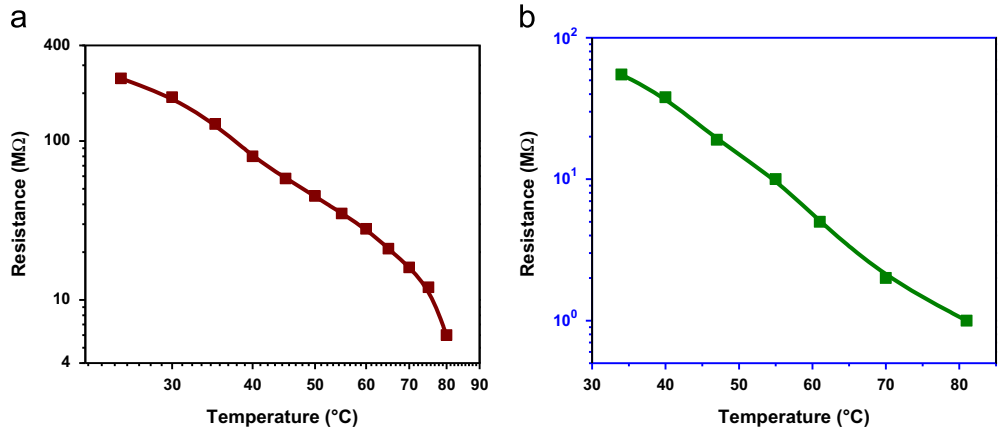

Fig. 5. Resistance–temperature relationships for the composite (a) and pure copper oxide (b).

Table 1
Electric parameters and compositions of the copper oxide composite and pure copper oxide based resistive temperature sensors.

Sr. no.	Composition	R_o (MΩ)	б ($\Omega^{-1}cm^{-1}$)	S (%/°C) (Temperature)	S (%/%RH) (Humidity)
1	CuO–Si-adhesive (Hero Gum) (1:1)	250	0.80×10^{-9}	−4.0	−2.9
2	Pure copper oxide press-tablets	55	0.22×10^{-6}	−5.2	−4.88

sensors. Table 1 shows the composition and electrical parameters of the sensors. As the response of the sensors is not linear, so, to linearize the resistance–temperature behavior the Log-resistance temperature relationship is drawn in Fig. 6 and this behavior is compared with straight line. It can be seen that the response of the sensor is near to linear.

For the explanation of conduction mechanism in temperature sensitive materials, the percolation theory may be used [36,37]:

$$б = 1/LZ \tag{2}$$

where б is the conductivity, L is the characteristic length, which depends on the concentration of sites and Z is the resistance of the path (Z) with the lowest average resistance. With increase in temperature the Z decreases, which results in increase in conductivity. The decrease in Z is because of generation of charge carriers as a result of increasing temperature [11].

The simulation of resistance–temperature behavior of the sensors is carried out by using the following mathematical function [38]:

$$f(x) = e^{-x} \tag{3}$$

The Eq. (3) has been modified as follows:

$$R/R_o = e^{-k\Delta T} \tag{4}$$

where R_o is initial resistance, R is resistance at elevated temperature, ΔT is change in temperature and k is the resistance temperature factor. The values of resistance temperature factor for CuO–Si-adhesive composite and pure copper oxide are 6.76×10^{-2} and 8.53×10^{-2} respectively. The comparison of experimental and simulated results is given in Fig. 7(a) and (b) for both types of sensors. It is evident from the graphs that the simulated results are in good agreement with experimental results.

The sensors are also characterized for humidity sensing. The humidity–capacitance behavior of sensor based on CuO–Si-adhesive composite is shown in Fig. 8(a), while the humidity–resistance behavior of sensors based on composite and pure copper oxide is shown on semi-logarithmic scale in Fig. 8(b) and Fig. 9,

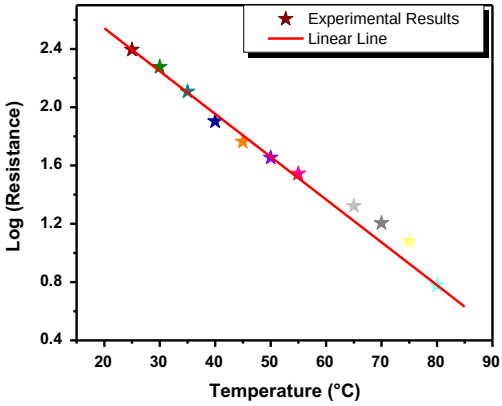

Fig. 6. Linearized resistance–temperature relationship of a sensor.

respectively. As shown in Fig. 9, the change in relative humidity (RH) from 38% to 90% causes to change the resistance up to 80 times in CuO-based sensor. The CuO–Si-adhesive composite based sensors show change in resistance and capacitance up to 845 times and 1395 times respectively for change in humidity from 47% to 95% RH. The humidity sensitivity of the sensors is calculated by using the following formula:

$$S = (\Delta R/R_o \Delta H)100 \tag{5}$$

where, R_o is initial resistance, while ΔR and ΔH are change in resistance and change in humidity respectively. The humidity sensitivity is found −2.9%/%RH and −4.88%/%RH, respectively for CuO–Si-adhesive and pure copper oxide based sensors.

The sensing mechanism is based on the change in capacitance and resistance with change in humidity. On exposing the sensors to the environment where humidity increases gradually, in the start at lower humidity the chemisorptions of water vapors takes place on the surface, while on further increase in humidity the physisorption takes place. In the lower range of humidity the sensors show large change in resistance, while small change in capacitance. The reasons for large change in resistance may be the donation of electron to metal oxide by chemisorption and ionic conduction because of little absorption of water. As humidity increases the physiosorption starts, the water molecules start to condensed on the surface in layer by layer fashion. During this stage initially chemisorbed and first physisorbed layers contribute in conduction by tunneling between donor H_2O sites and electron hopping along the surface of composite, while the further condensation results in protonic conduction and the rate of change of resistance becomes small. The physisorption also increases the

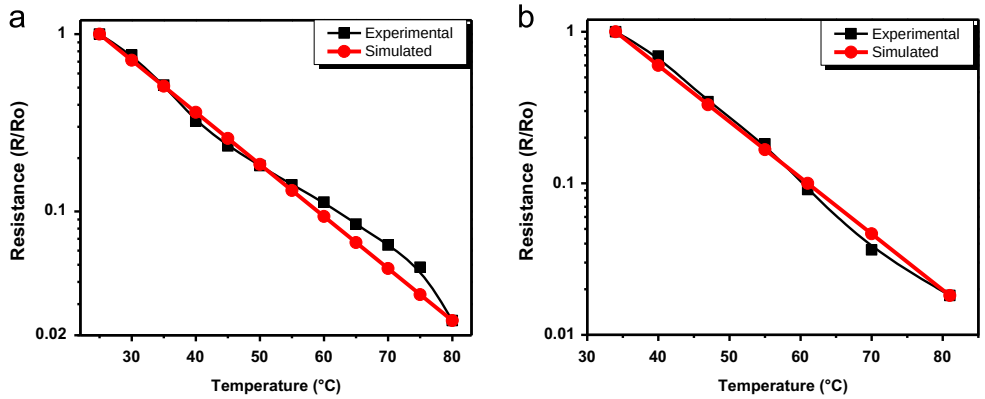

Fig. 7. The comparison of experimental and simulated results of composite (a) and pure copper oxide (b) based sensors.

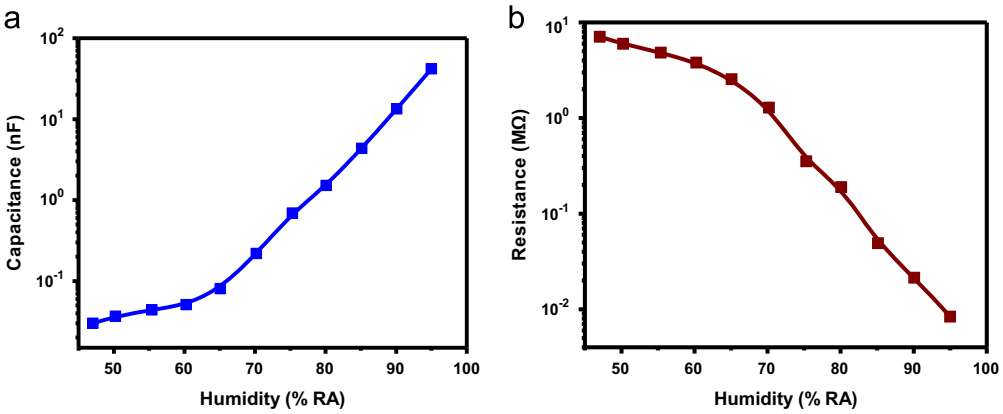

Fig. 8. Humidity–capacitance (a) and humidity–resistance (b) behavior of sensor based on CuO–Si-adhesive composite.

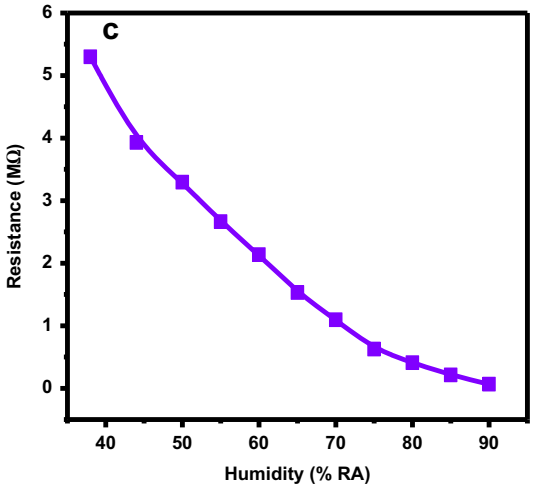

Fig. 9. Humidity–resistance behavior of sensor based on pure copper oxide.

rate of change of capacitance due to high dielectric constant of water [39–41].

There may be many other reasons for the increase in capacitance and decrease in resistance with increase in humidity; which include absorption of water molecule in the composite (that owing to displacement current reduces the resistance and augments the capacitance), doping of composite and development of charge transfer complexes [5,42–43]. Moreover, numerous other factors that affect the sensor's capacitance are area of electrodes, gap between electrodes and thin films material's dielectric constant. The capacitance also depends upon material's polarizability, basis of that are dipolar (α_{dip}), electronic (α_e), and ionic (α_i) [44]. In addition, at normal conditions the transfer of charge carriers (electrons and holes) is source of polarizability as well [38,42,45]. On the basis of sensor response, it is assumed that by the absorption of water molecules in the composite layer the dipolar polarizability of the sensor increases.

4. Conclusions

The humidity and temperature sensors based on pure copper oxide nanosheets and its composite with Si-adhesive have been fabricated and investigated. The $\sim 80 \pm 10$ nm thick copper oxide nanosheets are synthesized by low temperature stirring method and characterized by using FESEM, XRD and FTIR. Investigations of the electric properties of sensors reveal that the mechanism of temperature sensing is based on change in resistance, while that of humidity sensing is based on change in resistance as well as capacitance. With increase in temperature, the resistance decreases, that is attributed to the generation of charge carriers. The temperature sensitivity is $-5.2\%/^{\circ}C$ and $-4.0\%/^{\circ}C$ respectively for sensors based on pure copper oxide and its composites, that is comparable with sensitivity of the commercially available thermistors. Accordingly the humidity sensitivity of copper oxide–Si-adhesive composite and pure copper oxide nanosheets is $-2.9\%/\%$ RH and $-4.88\%/\%RH$ respectively. The fabricated sensors have great potential to use as humidity and temperature sensing element in the meters that may be used for the monitoring of humidity and temperature.

Acknowledgment

This project was funded by (SABIC) and the Deanship of Scientific Research (DSR), King Abdulaziz University, Jeddah, under grant no. MS/168/12/1433. The authors, therefore, acknowledge with thanks SABIC and DSR technical and financial support.

References

[1] N. Horzum, D. Taşçıoglu, S. Okur, M.M. Demir, Talanta 85 (2011) 1105–1111.
[2] H. Lam, G. Rao, J. Loureiro, L. Tolosa, Talanta 84 (2011) 65–70.
[3] S. Park, J. Kang, J. Park, S. Mun, Sensor Actuat. B-Chem. 76 (2001) 322–326.
[4] N. Camaioni, G. Casalbore-Miceli, Y. Li, M.J. Yang, A. Zanelli, Sensor Actuat. B-Chem. 134 (2008) 230–233.
[5] M.T.S. Chani, K.S. Karimov, F.A. Khalid, S.A. Moiz, Solid State Sci. 18 (2013) 78–82.
[6] M.V. Fuke, P. Kanitkar, M. Kulkarni, B.B. Kale, R.C. Aiyer, Talanta 81 (2010) 320–326.
[7] R. Nohria, R.K. Khillan, Y. Su, R. Dikshit, Y. Lvov, K. Varahramyan, Sensor Actuat. B-Chem. 114 (2006) 218–222.
[8] A.T. Ramaprasad, V. Rao, Sensor Actuat. B-Chem. 148 (2010) 117–125.
[9] J. Huang, Y. Hao, H. Lin, D. Zhang, J. Song, D. Zhou, Mater. Sci. Eng. B 99 (2003) 523–526.
[10] S.K. Mahadeva, S. Yun, J. Kim, Sensor Actuat. A-Phys. 165 (2011) 194–199.
[11] H.T. Hsueh, T.J. Hsueh, S.J. Chang, F.Y. Hung, T.Y. Tsai, W.Y. Weng, C.L. Hsu, B.T. Dai, Sensor Actuat. B-Chem. 156 (2011) 906–911.
[12] M.T.S. Chani, K.S. Karimov, F.A. Khalid, S.Z. Abbas, M.B. Bhatty, Chin. Phys. B 22 (2013) 010701-1–010701-6.
[13] K.S. Karimov, M. Saleem, Z.M. Karieva, A. Mateen, M. Tariq Saeed Chani, Q. Zafar, J. Condu. 33 (2012) 073001–073005.
[14] P.-G. Su, L.-N. Huang, Sensor Actuat. B-Chem. 123 (2007) 501–507.
[15] S. Zaman, M.H. Asif, A. Zainelabdin, G. Amin, O. Nur, M. Willander, J. Electroanal. Chem. 662 (2011) 421–425.
[16] M. Hübner, C.E. Simion, A. Tomescu-Stănoiu, S. Pokhrel, N. Bârsan, U. Weimar, Sensor. Actuat. B-Chem. 153 (2011) 347–353.
[17] M.K. Verma, V. Gupta, Sensor Actuat. B-Chem. 166–167 (2012) 378–385.
[18] L. Wang, Y. Kang, Y. Wang, B. Zhu, S. Zhang, W. Huang, S. Wang, Mater. Sci. Eng. C 32 (2012) 2079–2085.
[19] Q. Qi, T. Zhang, Y. Zeng, H. Yang, Sensor Actuat. B-Chem. 137 (2009) 21–26.
[20] D.P. Dubal, G.S. Gund, R. Holze, C.D. Lokhande, J. Power Sour. 242 (2013) 687–698.
[21] M. Faisal, S.B. Khan, M.M. Rahman, A. Jamal, A. Umar, Mater. Lett. 65 (2011) 1400–1403.
[22] Y. Liu, Y. Qiao, W. Zhang, P. Hu, C. Chen, Z. Li, L. Yuan, X. Hu, Y. Huang, J. Alloy Compd. 586 (2014) 208–215.
[23] M.M. Rahman, S.B. Khan, A.M. Asiri, H.M. Marwani, A.H. Qusti, Compos. Part-B Eng. 54 (2013) 215–223.
[24] L. Tian, B. Liu, Appl. Surf. Sci. 283 (2013) 947–953.
[25] Q. Zhang, K. Zhang, D. Xu, G. Yang, H. Huang, F. Nie, C. Liu, S. Yang, Prog. Mater. Sci. 60 (2014) 208–337.
[26] X.H. Huang, X.H. Xia, Y.F. Yuan, F. Zhou, Electrochim. Acta 56 (2011) 4960–4965.
[27] C. Robert, A. Crespy, S. Bastide, J.M. Lopez-Cuesta, S. Kerboeuf, C. Artigue, E. Grard, Int. J. Adhes. Adhes. 24 (2004) 55–68.
[28] G. Tolia, S. Kevin Li, Eur. J. Pharm. Biopharm. 82 (2012) 518–525.
[29] M.T.S. Chani, K.S. Karimov, F. Ahmad Khalid, K. Raza, M. Umer Farooq, Q. Zafar, Physica E 45 (2012) 77–81.
[30] K.S. Karimov, F.A. Khalid, M.T.S. Chani, Measurement 45 (2012) 918–921.
[31] K. Sanginovich Karimov, M.T. Saeed Chani, F. Ahmad Khalid, A. Khan, Physica E 44 (2012) 778–781.
[32] S.B. Khan, M. Faisal, M.M. Rahman, I.A. Abdel-Latif, A.A. Ismail, K. Akhtar, A. Al-Hajry, A.M. Asiri, K.A. Alamry, New J. Chem. 37 (2013) 1098–1104.
[33] R.A. Zarate, F. Hevia, S. Fuentes, V.M. Fuenzalida, A. Zúñiga, J. Solid State Chem. 180 (2007) 1464–1469.
[34] J.W. Dally, W. Riley, K.G. McConnell, Instrumentation for Engineering Measurements, John Wiley and Sons Inc, New York, 1993.
[35] R.L. Boylestad, L. Nashelsky, L. Li, Electronic Devices and Circuit Theory, Prentice-Hall, New Jersey, 2006.
[36] H. Bottger, V.V. Bryksin, Hopping Conduction in Solids, VCH, Deerfield Beach, FL, 1985.
[37] C. Brabec, J.P.a.N.S.V. Dyakonov, Organic Photovoltaics: Concepts and Realization, Springer-Verlag, Berlin Heidelberg, 2003.
[38] A. Croft, T. Croft, R. Davison, M. Hargreaves, Engineering Mathematics: a Modern Foundation for Electronic, Electrical, and Control Engineers, Addison-Wesley, London, 1992.
[39] Z. Chen, C. Lu, Sensor Lett. 3 (2005) 274–295.
[40] K.M.S. Khalil, S.A. Makhlouf, Sensor Actuat. A-Phys. 148 (2008) 39–43.
[41] Q. Yuan, N. Li, W. Geng, Y. Chi, J. Tu, X. Li, C. Shao, Sensor Actuat. B-Chem. 160 (2011) 334–340.
[42] S.N. Boguslavsky, V.V. Vannikov, Organic Semiconductors, V.A. Kargin, Nauka, Moscow, 1968.
[43] S.A. Moiz, M.M. Ahmed, K.S. Karimov, Jpn. J. Appl. Phys. 44 (2005) 1199–1203.
[44] M.A. Omar, Elementary Solid State Physics: Principles and Applications, Pearson Education (Singapore) Pt. Ltd., Indian branch, Delhi, India, 2002.
[45] M. Iwamoto, T. Manaka, IPAP Conf. Ser. 6 (2005) 63–68.